Compound-Resolved Gas–Water Assessment of RDF Pyrolysis with Wet Scrubbing: Operating Windows for ICE-CHP and Closed-Loop Water Management

Sergejs Osipovs * and Aleksandrs Pučkins

Posted Date: 23 March 2026

doi: 10.20944/preprints202603.1829.v1

Keywords: refuse-derived fuel; pyrolysis; wet scrubbing; tar; BTEX; phenolics; PAHs; design of experiments

 doi:10.20944/preprints202603.1829.v1

Article

Compound-Resolved Gas–Water Assessment of RDF Pyrolysis with Wet Scrubbing: Operating Windows for ICE-CHP and Closed-Loop Water Management

Sergejs Osipovs * and Aleksandrs Pučkins

Daugavpils University; Daugavpils, Parades 1A, LV-5401, Latvia

* Correspondence: sergejs.osipovs@du.lv

Abstract

Pyrolysis of refuse-derived fuel (RDF) is a promising waste-to-energy route, but its use in higher-value applications remains limited by tar carryover, BTEX, heteroatom-containing compounds, and pollutant accumulation in recirculated scrubber water. This study evaluated operating windows for RDF pyrolysis coupled with direct wet scrubbing and closed-loop water reuse, with the aim of identifying regimes suitable for different end-use tiers. An L27 design of experiments was applied to 27 pyrolysis runs by varying pyrolysis temperature, residence time, scrubber liquid-to-gas ratio, scrubber-water temperature, and sequential reuse of the same scrubber-water inventory over 5, 10, and 15 cycles. Cleaned-gas pollutants were quantified by compound-resolved GC–MS after solid-phase adsorption sampling, while phenolics and PAHs in scrubber water were determined by extraction followed by GC–MS. The results showed that stronger scrubbing reduced gas-phase tar and BTEX burdens, whereas extended water reuse caused systematic accumulation of phenolics and PAHs and increased the composite water-loop hazard index. Boiler-grade operation remained feasible across a broad operating range, whereas ICE-CHP feasibility was restricted to a narrow robust regime and no robust microturbine-grade condition was identified. These findings show that operating windows for RDF pyrolysis must be defined jointly by gas-cleanliness and water-loop management constraints.

Keywords: refuse-derived fuel; pyrolysis; wet scrubbing; tar; BTEX; phenolics; PAHs; design of experiments

1. Introduction

Refuse-derived fuel (RDF) pyrolysis is increasingly considered a flexible waste-to-energy (WtE) pathway capable of converting heterogeneous residual waste streams into gaseous and liquid energy carriers while reducing landfill dependence and supporting circular-economy strategies [1,2]. Unlike single-stream biomass, RDF represents a compositional continuum in which fossil-derived fractions (plastics, rubber) coexist with biogenic fractions (paper/cardboard, wood, textiles of natural origin, and other renewable residues). When a relevant share of RDF is biogenic, the resulting energy output can contribute—under well-defined accounting boundaries and documented feed characterization—to renewable energy targets and decarbonization objectives [1]. However, the practical utilization of RDF-derived pyrolysis gas is constrained not only by conversion efficiency, but also by pollutant chemistry and its system-level consequences.

From an end-use perspective, RDF pyrolysis gas is not a single fuel but a complex mixture whose deployability depends on the concentration, volatility, and speciation of impurities. Condensable organics broadly referred to as tar, volatile aromatics such as benzene, toluene, ethylbenzene, and xylenes (BTEX), polycyclic aromatic hydrocarbons (PAHs), and heteroatom-containing species can compromise reliability, emissions performance, and downstream operability [3,4]. Foundational work and subsequent reviews emphasize that tar is not a single compound class, but a spectrum

 doi:10.20944/preprints202603.1829.v1

spanning oxygenated species and aromatic families of different volatility and reactivity; consequently, tar measurement, reporting comparability, and decision relevance remain non-trivial issues in thermochemical conversion research [4]. Accordingly, modern reviews consistently frame tar control and gas cleaning as enabling steps for implementation, particularly when the intended end-use requires stable long-duration operation [5–7]. In industrial pyrolysis streams, gas chromatography–mass spectrometry (GC–MS)-based workflows for tar quantification have also been developed and validated on real pyrolysis products, reinforcing the importance of method transparency and compound-resolved reporting for deployment-oriented conclusions [8].

End-use requirements strongly shape both the required level of gas conditioning and the identity of the limiting pollutant classes. For direct heat production in boilers, tolerance to residual condensables and aromatic burdens is typically higher, allowing less stringent gas cleaning. In contrast, internal combustion engine combined heat and power (ICE-CHP) generally requires substantially cleaner gas to prevent deposit formation, intake fouling, lubricant degradation, and unstable operation; engine-oriented studies and reviews consistently highlight stringent tar control as a prerequisite for stable internal combustion engine utilization of producer gas [9–11]. Performance-focused analyses further show that producer-gas quality strongly influences engine efficiency, operability, and long-term stability [10]. Microturbines may offer advantages in compactness and emissions control, yet they still require tight control of particulates and condensables to protect hot-section components and maintain stable combustion [12,13], and turbine-oriented studies explicitly identify gas cleaning as a decisive constraint for viable turbine operation on biomass- and waste-derived gases [14]. Consequently, upgrading RDF pyrolysis gas from combustible to engine- or turbine-compatible is fundamentally a pollutant-management and system-integration problem rather than merely an energy-conversion problem.

Among practical conditioning options, wet scrubbing remains one of the most widely applied steps in thermochemical conversion because of its mechanical simplicity, rapid quench capability, and scalability. Recent studies and reviews of wet scrubbing for producer-gas cleaning show that cooling, condensation, and mass transfer to the liquid phase can reduce the carryover of condensable and aerosol-associated species, with performance strongly influenced by operating parameters such as the liquid-to-gas ratio (L/G), liquid temperature, and contacting configuration [15–17]. For RDF-derived vapors, a direct water scrubber can therefore reduce condensable and droplet-associated pollutant transport to the downstream user by redistributing part of the burden from the gas phase to the liquid phase [15–17]. However, this advantage introduces a coupled constraint: wet scrubbing does not eliminate pollutants; it redistributes them. As scrubbing intensity increases, pollutant burden shifts from the cleaned gas into the scrubbing liquid, where it can accumulate under recirculation. Consecutive operation using the same scrubber-water inventory can therefore lead to measurable build-up of organic pollutants, altered class distributions, and increased hazard and disposal burdens, making water-loop management (purge/make-up and/or treatment) a co-equal design constraint alongside gas quality [18].

This coupling becomes especially critical under repeated operation. When the same scrubber-water volume is reused across multiple consecutive pyrolysis runs, soluble and semi-volatile organic fractions can accumulate rapidly, and the composition can drift toward more persistent and higher-molecular-weight species. Such “heavification” trends and speciation shifts are consistent with tar literature discussing how downstream units can alter tar class distributions and enrich PAH-like fractions under certain configurations [4,19,20]. Pollutant behavior is also strongly class-dependent. BTEX and other light aromatics are comparatively volatile and may respond only partially to water-based scrubbing, whereas phenolics and heavier condensables can transfer more efficiently to the liquid phase; PAHs may be captured effectively through condensation and droplet or aerosol mechanisms, but they can also accumulate disproportionately in recirculated media [3,4,15]. Heteroatom markers, including N-heterocycles and S-aromatics, matter not only as emissions precursors, but also as indicators of corrosion- and catalyst-relevant burdens when downstream cleanup or aftertreatment is considered [3,15]. Accordingly, compound-resolved analytics are

 doi:10.20944/preprints202603.1829.v1

essential to translate gas cleaning into end-use-relevant risk metrics and deployment-oriented feasible regimes rather than relying on total tar alone [9,21–23].

Despite extensive literature on tar mitigation and gas cleaning, three gaps remain particularly relevant for RDF with variable biogenic fraction and simple wet-scrubbing architectures: (i) limited multi-factor design-of-experiments (DOE)-based experimental mapping that couples pyrolysis severity with direct wet-scrubber setpoints; (ii) insufficient treatment of recirculated scrubber water as a co-equal constraint alongside gas quality, especially under explicitly defined sequential cycles; and (iii) a lack of robust operating guidance that remains valid when the biogenic fraction varies within realistic bounds [1–4,15]. In this work, we address these gaps through an experimental L27 DOE campaign (27 pyrolysis runs) that couples pyrolysis severity (temperature and residence time) with direct water-scrubber operation (L/G and scrubber-water temperature) and closed-loop behavior represented by 5, 10, and 15 consecutive pyrolysis cycles using the same scrubber-water volume. Cleaned-gas pollutant classes were quantified by compound-resolved GC–MS using a solid-phase adsorption (SPA) sampling approach, while scrubber-water phenolics and PAHs were quantified by extraction followed by GC–MS [1,24–27]. The study identifies operating windows jointly constrained by gas-side cleanliness and water-loop manageability and shows that feasible operating space contracts sharply as end-use requirements tighten, with water-loop accumulation becoming a decisive constraint under extended cycling.

2. Materials and Methods

2.1. Rotary-Kiln RDF Pyrolysis System and L27 DOE Operating Matrix

RDF pyrolysis experiments were carried out in a pilot-scale system integrating a rotary-kiln pyrolyzer with a direct water scrubber for primary gas cleaning. The experimental unit is located in Daugavpils, Latvia, and is based on a horizontal rotating-drum configuration with a nominal throughput of up to 9 t day^{-1}. The kiln was manufactured from stainless steel and operated in cyclic mode at a fixed rotation speed of $\omega = 0.15$ rad s^{-1}. The feedstock was refuse-derived fuel (RDF), and feed variability was represented by three biogenic-fraction categories (40, 50, and 60 wt%), reflecting realistic fluctuations in mixed waste-derived fuels (Figure 1).

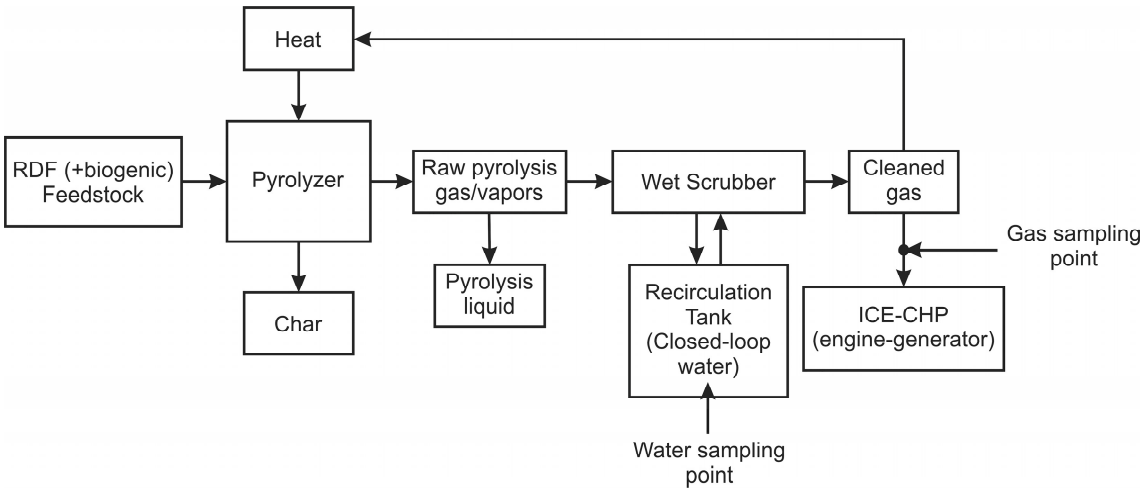

Figure 1. Schematic of the RDF with a variable biogenic fraction pyrolysis line coupled with a direct wet scrubber operated with closed-loop water recirculation. The cleaned-gas sampling point (post-scrubber) and the scrubber-water sampling point (recirculation tank) used for compound-resolved GC–MS analysis are indicated.

A structured L27 orthogonal design of experiments (DOE) was implemented to evaluate the combined effects of pyrolysis severity and wet-scrubber operating conditions on pollutant burdens in the cleaned gas and in the recirculating scrubber water. The controllable DOE factors were

 doi:10.20944/preprints202603.1829.v1

pyrolysis temperature (T_{pyro} = 380, 450, and 520 °C), effective residence time (τ = 5, 15, and 30 min), scrubber liquid-to-gas ratio (L/G = 0.5, 1.0, and 2.0 L m^{-3}), and scrubber-water temperature (T_{scrub} = 20, 35, and 50 °C). The 27 operating conditions are listed in Table 1.

Table 1. L27 DOE operating matrix for RDF pyrolysis and direct wet scrubbing.

Run	T_{pyro} (°C)	Residence time, τ (min)	Scrubber L/G (L m^{-3})	Scrubber T (°C)	Sequential cycles (n)
1	380	5	0.5	20	5
2	380	5	1	20	10
3	380	5	2	20	15
4	380	15	0.5	35	15
5	380	15	1	35	5
6	380	15	2	35	10
7	380	30	0.5	50	10
8	380	30	1	50	15
9	380	30	2	50	5
10	450	5	0.5	35	10
11	450	5	1	35	15
12	450	5	2	35	5
13	450	15	0.5	50	5
14	450	15	1	50	10
15	450	15	2	50	15
16	450	30	0.5	20	15
17	450	30	1	20	5
18	450	30	2	20	10
19	520	5	0.5	50	15
20	520	5	1	50	5
21	520	5	2	50	10
22	520	15	0.5	20	10
23	520	15	1	20	15
24	520	15	2	20	5
25	520	30	0.5	35	5
26	520	30	1	35	10
27	520	30	2	35	15

The closed-loop reuse state of the scrubber-water inventory was evaluated at 5, 10, and 15 consecutive pyrolysis cycles using the same water volume. In this study, cycle number was treated as a state variable describing pollutant accumulation in the recirculating liquid phase rather than as an independently randomized operating factor. This approach allowed the combined assessment of gas-side cleanliness and water-loop pollutant build-up under repeated operation.

Each pyrolysis run was treated as a 1.0 h cycle with an RDF feed mass of 400 kg per run, corresponding to a nominal throughput of approximately 0.4 t h^{-1}. The direct water scrubber was operated with a recirculating water inventory of 1.0 m^3. During the 5/10/15-cycle sequences, the same scrubber-water inventory was reused without deliberate purge or blowdown; only minor make-up water was added to compensate for evaporation and handling losses, typically ≤1–3% per cycle.

After each run, or at defined points within a sequential cycle series, samples of (i) cleaned gas downstream of the scrubber and (ii) scrubber water from the recirculation tank and/or scrubber outlet were collected for compound-resolved analysis (Sections 2.4–2.7). This experimental design made it possible to identify operating windows constrained simultaneously by end-use-relevant gas quality and by pollutant accumulation in the water loop under repeated closed-loop operation.

 doi:10.20944/preprints202603.1829.v1

2.2. Pollutant Classes and Representative Compounds

The analytical dataset resolves pollutant classes relevant to downstream engine operability and to scrubber-water manageability under closed-loop operation. The light-aromatic fraction was represented by BTEX-related compounds, including benzene, toluene, xylenes, and styrene, reported both as selected individual compounds and as a class sum. Phenolic species were represented by phenol, cresols, and xylenols. The PAH fraction covered compounds from naphthalene (2-ring) to heavier PAHs, including pyrene- and chrysene-class compounds, and was additionally summarized using a heavy-PAH index. Nitrogen-containing aromatic markers were represented by quinoline-class heterocycles, while sulfur-containing aromatic markers were represented by thiophene- and benzothiophene-class compounds. These classes were selected because they jointly describe gas-cleanliness constraints for end-use applications and pollutant accumulation trends in the recirculating scrubber water.

2.3. Feedstock Variability and Biogenic-Fraction Categorization (40/50/60 wt%)—Mass-Fraction Approach

In addition to the 27-run DOE matrix, feedstock variability was incorporated through three discrete RDF biogenic-fraction categories (40, 50, and 60 wt%), representing realistic variation in the renewable share of mixed waste-derived fuel. The biogenic fraction of each RDF batch was estimated using a mass-fraction (morphological) approach in which the incoming RDF was manually sorted into predefined material groups, each fraction was weighed, and a biogenic share was assigned based on material origin.

Representative RDF subsamples were collected from each batch (n = 3 subsamples per batch; 1–5 kg per subsample). The subsamples were sorted into material categories such as paper/cardboard, wood and textiles of natural origin, food/organic residues, plastics, rubber, metals, glass/inert material, and fines. The wet mass of each fraction was recorded and, where required, fractions were dried at 105 °C to constant mass to obtain dry-basis mass fractions. The overall biogenic mass fraction on a dry basis was then calculated according to Equation (1), where m_i is the dry-basis mass of material fraction i, and the numerator includes all fractions classified as biogenic.

$$w_{bio} = \frac{\sum m_i(\text{biogenic fractions})}{\sum m_i\ (\text{all fractions})} \quad (1)$$

Each batch was assigned to the nearest biogenic-fraction category (40, 50, or 60 wt%) using a tolerance band of ±2–5 wt%, based on between-subsample variability. The resulting category label was propagated through the DOE dataset and used in the subsequent feasibility screening. For cross-category comparability, each batch or category was additionally characterized in terms of proximate/ultimate composition and key heteroatom- and ash-forming elements, including Cl, S, and N. These supporting data were used to interpret category-dependent changes in pollutant formation and phase partitioning, including shifts in oxygenated species, phenolics, BTEX, PAH profiles, and N/S marker indices.

Operating windows were classified as robust when the screening constraints were satisfied across all three biogenic-fraction categories under otherwise comparable process setpoints, thereby reflecting resilience to realistic RDF composition variability encountered in practice. The morphological sorting results were therefore used both to assign each RDF batch to the Bio 40/50/60 wt% categories and to label the corresponding DOE runs used in the Results and operating-window screening.

2.4. Sample Preparation

Samples of recirculated scrubber water and cleaned pyrolysis gas were prepared for compound-resolved GC–MS analysis as described below.

 doi:10.20944/preprints202603.1829.v1

2.4.1. Scrubber-Water Sample Preparation (Extraction Before GC–MS)

Recirculated scrubber water was sampled in triplicate after 5, 10, and 15 consecutive pyrolysis cycles performed using the same scrubber-water inventory. Samples were collected from the recirculation tank and, where relevant, from the scrubber outlet, transferred into pre-cleaned amber glass bottles fitted with PTFE-lined caps, cooled immediately, and stored at 4 °C protected from light. Extraction was performed as soon as practical, typically within 24–48 h of sampling.

Phenolics and PAHs were extracted by liquid–liquid extraction (LLE) using dichloromethane (DCM). For each replicate, 100 mL of scrubber water was transferred into an extraction vessel and spiked with surrogate standards before extraction to enable recovery tracking. The sample was extracted with 4 mL of DCM by vigorous shaking for 30 min. This extraction step was repeated three times using the same aqueous aliquot in order to improve analyte recovery. The organic phases were combined, dried over anhydrous Na_2SO_4, and concentrated under reduced pressure by rotary evaporation to a fixed final volume, typically 0.5–1.0 mL. The final extract was filtered through a PTFE syringe filter (0.22–0.45 μm) into an autosampler vial, and internal standards were added immediately before GC–MS injection to normalize instrument response and support quantification.

2.4.2. Cleaned-Gas Sample Preparation (SPA Sampling and Solvent Desorption Before GC–MS)

Cleaned pyrolysis gas downstream of the direct water scrubber was sampled using a two-stage solid-phase adsorption (SPA) train designed to capture both condensable or semi-volatile tar components and volatile aromatics. The sampling train consisted of an aminopropyl-bonded silica cartridge as the primary stage and an activated-carbon cartridge as the secondary stage for the more volatile fraction (Figure 2). The sampling configuration and its suitability for the simultaneous capture of tar-related compounds and BTEX were adopted from our validated SPA protocol [23,28–32].

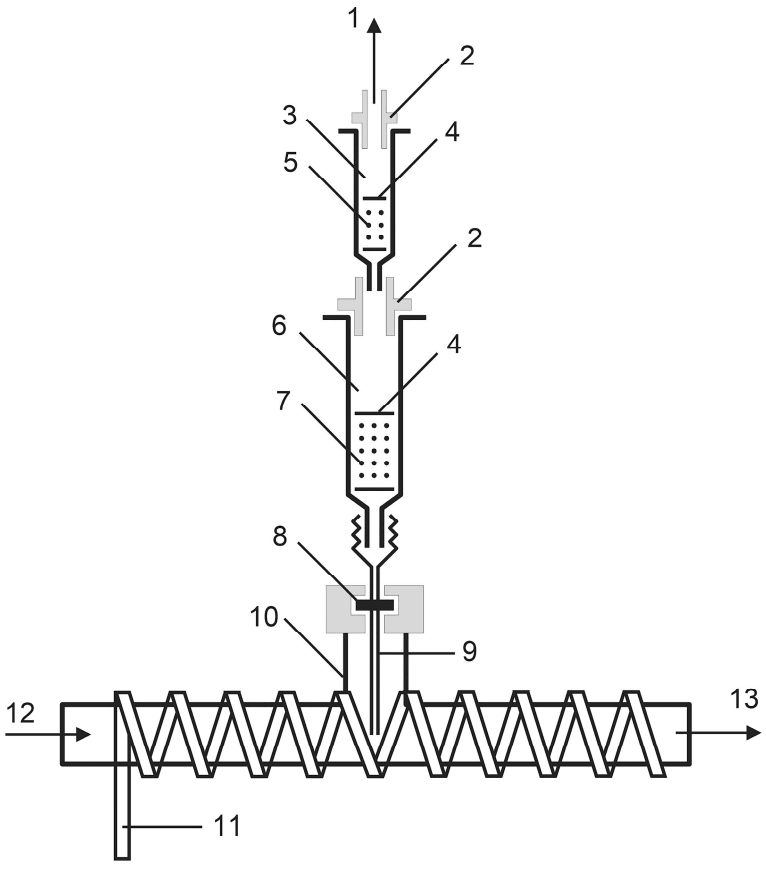

Figure 2. Schematic of the sampling device used for tar collection from the cleaned pyrolysis gas. 1. pump connection; 2. adapter; 3. second sorbent column; 4. fritted disc; 5. activated coconut charcoal; 6. first sorbent

 doi:10.20944/preprints202603.1829.v1

column; 7. amino-phase sorbent; 8. rubber/silicone septum; 9. needle; 10. glass T tube; 11. heating tape; 12. product gas inlet; 13. connection to an electric pump.

To minimize condensation artefacts upstream of the sorbent cartridges, the sampling T-piece and transfer line were heated to approximately 250 °C using insulated heating tape. Gas was drawn through the heated line at approximately atmospheric pressure using a sampling pump operated at a constant flow rate of 100 mL min^{-1}, and the total sampled volume was recorded for each replicate.

Nitrogen- and sulfur-containing aromatic markers were sampled using the same heated transfer line and two-stage SPA configuration. In this arrangement, less volatile and more strongly interacting N/S species were retained predominantly on the NH_2 stage, whereas more volatile N/S aromatics were captured more efficiently on the activated-carbon stage [33]. For the calculation of the composite indices I_N and I_S, marker masses quantified in the NH_2-stage extract and in the carbon-stage extract were combined and normalized to the sampled gas volume, reported in mg Nm^{-3} under normal conditions. Breakthrough or redistribution between stages was evaluated by comparing marker responses in the two cartridges. As a QC criterion, the second-stage contribution was required to remain ≤10% of the first-stage mass for representative markers; otherwise, the sample was flagged as potentially affected by breakthrough.

After sampling, both cartridges were sealed immediately to minimize evaporative losses and prevent contamination. Compounds retained on the NH_2 cartridge were eluted with three successive 600 µL portions of a 1:1 (v/v) dichloromethane/acetonitrile mixture into pre-cleaned GC vials. The fractions were combined in a single vial, and internal standards were then added at a fixed volume using a calibrated micropipette. Compounds retained on the activated-carbon cartridge were desorbed separately with 1.0 mL of carbon disulfide (CS_2) under intermittent agitation for at least 30 min. Internal standards were added to both the NH_2-stage and carbon-stage extracts before GC–MS analysis, enabling direct comparison of the primary and backup stages during breakthrough assessment.

For data processing, the two extracts were treated as complementary fractions of the same gas sample. The NH_2-stage extract was used primarily for semi-volatile and more strongly retained compounds, including phenolics and higher aromatic species, whereas the activated-carbon extract captured the most volatile aromatics, predominantly BTEX. Compound-class sums and derived indices were calculated by combining the mass contributions from both stages after blank correction and replicate averaging. In practice, BTEX quantification was derived mainly from the activated-carbon stage, whereas heavier tar- and PAH-related indices were dominated by the NH_2-stage.

2.5. GC–MS Analysis

GC–MS analyses were performed using a Shimadzu GCMS-QP2010 system (Shimadzu Corporation, Kyoto, Japan) equipped with an electronically controlled split/splitless injector. Chromatographic separation was achieved on a fused-silica capillary column (Restek Rtx-5SIL-MS, 30 m × 0.32 mm i.d., 0.25 µm film; 5% diphenyl/95% dimethylpolysiloxane). Helium (99.999%) was used as the carrier gas at a constant flow rate of 1.6 mL min^{-1}.

Samples (1 µL) were injected at 250 °C in split mode with a split ratio of 1:10. The oven temperature program was as follows: 30 °C for 5 min, ramped to 180 °C at 10 °C min^{-1}, then to 300 °C at 15 °C min^{-1}, followed by a final hold at 300 °C for 5 min. The mass spectrometer was operated in electron ionization (EI) mode at 70 eV. The ion source and transfer-line temperatures were maintained at 200 °C and 310 °C, respectively. Data acquisition was performed in selected ion monitoring (SIM) mode.

Target compounds were identified using retention-time matching together with qualifier/quantifier ion-ratio checks within the validated SIM method. The analytical method was applied to both cleaned-gas extracts obtained by solid-phase adsorption sampling and scrubber-water extracts obtained after liquid–liquid extraction.

 doi:10.20944/preprints202603.1829.v1

2.6. Calibration and Quantification

Quantified target compounds and their calibration parameters are summarized in Table 2. Quantification was based on internal-standard normalization and external calibration. tert-Butylcyclohexane and 4-ethoxyphenol were used as internal standards for aromatic hydrocarbons and phenolic compounds, respectively.

Table 2. Mass spectrometric data and LOD for quantified tar and internal standards.

No.	Compound	Chemical formula	Molecular weight, g mol^{-1}	Mass spectrum (NIST 20), mass (abundance)	LOD, ng
1	Benzene	C_6H_6	78	78 (999), 77 (283), 51 (221)	0.0032
2	Toluene	C_7H_8	92	91 (999), 92 (776), 65 (121)	0.0046
3	m-p-Xylene	C_8H_{10}	106	-	0.0051
4	o-Xylene	C_8H_{10}	106	91 (999), 106 (501), 105 (206)	0.0077
5	Phenol	C_6H_6O	94	94 (999), 66 (387), 65 (266)	0.0106
6	tert-Butylcyclohexane	$C_{10}H_{20}$	140	56 (999), 57 (674), 41 (236)	-
7	4-Ethoxyphenol	$C_8H_{10}O_2$	138	110 (999), 138 (333), 81 (299)	-
8	Indane	C_9H_{10}	118	117 (999), 118 (692), 115 (266)	0.0035
9	Indene	C_9H_8	116	116 (999), 115 (792), 89 (100)	0.0077
10	o-Cresol	C_7H_8O	108	108 (999), 107 (673), 79 (253)	0.0089
11	m-p-Cresol	C_7H_8O	108	-	0.0094
12	Naphthalene	$C_{10}H_8$	128	128 (999), 129 (109), 127 (107)	0.0033
13	Acenaphthylene	$C_{12}H_8$	152	152 (999), 153 (152), 151 (137)	0.0092
14	Acenaphthene	$C_{12}H_{10}$	154	153 (999), 154 (827), 152 (507)	0.0112
15	9H-Fluorene	$C_{13}H_{10}$	166	166 (999), 165 (844), 167 (140)	0.0045
16	Phenanthrene	$C_{14}H_{10}$	178	178 (999), 176 (202), 179 (150)	0.0148
17	Anthracene	$C_{14}H_{10}$	178	178 (999), 179 (156), 176 (140)	0.0182
18	Fluoranthene	$C_{16}H_{10}$	202	202 (999), 203 (173), 200 (153)	0.0066
19	Pyrene	$C_{16}H_{10}$	202	202 (999), 203 (170), 200 (152)	0.0081
20	Chrysene	$C_{18}H_{12}$	228	228 (999), 226 (271), 229 (203)	0.0050
21	Benzo(a)pyrene	$C_{20}H_{12}$	252	252 (999), 253 (215), 250 (172)	0.0047

Calibration mixtures were prepared from neat reference standards of the target analytes. A fixed and known amount of the corresponding internal standard was added to each calibration solution and to all study samples. Peak areas were integrated and normalized to the internal-standard response prior to regression analysis.

Calibration curves were constructed using five concentration levels (0.5, 1, 5, 20, and 50 ng per injection), with each level prepared and analyzed in triplicate. Linear regression with 1/x weighting was applied to improve quantification accuracy at low concentration levels while maintaining adequate performance over the full working range. Calibration was accepted when the coefficient of determination was $R^2 \geq 0.995$ and back-calculated concentrations were within ±15% of the nominal value, or within ±20% at the lowest calibration level.

For compounds detected in the chromatograms but not included in the calibrated target list, concentrations were estimated using the response factor of the calibrated compound with the closest retention time within the same chemical class. Total tar concentration in the cleaned gas was calculated as the sum of all identified, quantified, and response-factor-estimated tar-related compounds included in the tar-proxy definition. For scrubber-water extracts, concentrations were corrected using extraction-recovery factors obtained during QA/QC evaluation.

The instrumental limit of detection (LOD) was determined directly from chromatograms using a signal-to-noise ratio of 3 (S/N = 3). Compound-specific LOD values are reported in Table 2.

 doi:10.20944/preprints202603.1829.v1

2.7. Metrics and Operating-Window Definition

To translate compound-resolved pollutant measurements into deployment-oriented feasible regimes, two primary response groups were evaluated: (i) cleaned-gas quality metrics relevant to end-use operability, and (ii) water-loop manageability metrics relevant to sequential closed-loop scrubber-water reuse. Gas-side assessment was based on the cleaned-gas tar proxy (C_{tar}), the BTEX class sum (C_{BTEX}), and the nitrogen- and sulfur-marker indices (I_N and I_S). Water-loop assessment was based on phenolic and PAH accumulation in the recirculated scrubber water and on a composite dimensionless hazard proxy, I_{tox}, designed to represent the manageability of the closed-loop scrubber-water inventory under repeated reuse (see Section 2.7.2).

Operating windows were defined by identifying DOE conditions that satisfied both gas-side and water-side constraints for a given end-use tier. Because acceptable pollutant burdens differ substantially among boilers, internal combustion engine combined heat and power (ICE-CHP) systems, and microturbines, feasibility screening was performed using a tiered framework with progressively stricter thresholds (see Section 2.7.1). These thresholds are used here as transparent engineering screening criteria for comparative feasibility mapping within the tested operating space and are not presented as OEM certification limits.

2.7.1. Operating-Window Screening (Tiered End-Use Targets)

To enable deployment-oriented interpretation of the experimental results, three end-use tiers were defined:

- Tier A: boiler-grade utilization;
- Tier B: ICE-CHP utilization;
- Tier C: microturbine-oriented utilization.

Gas-side feasibility was assessed using the cleaned-gas indices C_{tar}, C_{BTEX}, I_N, and I_S. The corresponding tier-specific screening targets are summarized in Table 3.

Table 3. Gas-side screening targets for tiered end-use evaluation (cleaned gas; mg Nm^{-3}).

End-use tier	C_{tar}	C_{BTEX}	I_N	I_S
Tier A — Boiler	≤ 6000	≤ 3000	≤ 70	≤ 90
Tier B — ICE-CHP	≤ 2500	≤ 1600	≤ 40	≤ 55
Tier C — Microturbine	≤ 1000	≤ 800	≤ 25	≤ 35

These gas-side thresholds were selected to provide a consistent comparative basis for screening across the three end-use tiers. Where direct manufacturer specifications were unavailable, threshold values were selected within literature-reported ranges for producer-gas conditioning and for engine- and turbine-oriented gas-quality requirements.

Water-loop feasibility was assessed using the composite hazard proxy I_{tox}, which integrates phenolic, total PAH, and heavy-PAH burdens in the recirculated scrubber water under sequential reuse of the same water inventory. Tier-specific I_{tox} limits are summarized in Table 4.

Table 4. Water-loop hazard screening limits for sequential closed-loop operation (dimensionless).

End-use tier	I_{tox}
Tier A — Boiler	≤ 12.0
Tier B — ICE-CHP	≤ 9.0
Tier C — Microturbine	≤ 7.5

A DOE condition was classified as feasible within a given tier only if both the gas-side criteria (Table 3) and the corresponding water-loop criterion (Table 4) were satisfied at the sequential cycling level associated with that run (5, 10, or 15 consecutive cycles; see Table 1). A condition was classified

 doi:10.20944/preprints202603.1829.v1

as robust when feasibility was retained across all three experimentally categorized RDF biogenic-fraction groups (40, 50, and 60 wt%).

For transparency, the ICE-CHP-oriented screening outcomes across all DOE runs and all three biogenic-fraction categories are summarized in Table 5.

Table 5. ICE-CHP (Tier B) operating-window screening outcomes across RDF biogenic-fraction categories (Bio 40/50/60 wt%).

Run	Feasible (Bio 40%)	Feasible (Bio 50%)	Feasible (Bio 60%)	n/3 feasible	Robust (all Bio 40/50/60)	Primary limiting factor	Max normalized exceedance
1	N	N	N	0	N	Gas-side C_{tar}	3.47
2	N	N	N	0	N	Gas-side C_{tar}	3.18
3	N	N	N	0	N	Water-loop I_{tox}	3.62
4	N	N	N	0	N	Gas-side C_{tar}	2.94
5	N	N	N	0	N	Gas-side C_{tar}	2.71
6	N	N	N	0	N	Gas-side C_{tar}	3.05
7	N	N	N	0	N	Gas-side C_{tar}	2.58
8	N	N	N	0	N	Gas-side C_{tar}	2.84
9	N	N	N	0	N	Gas-side C_{tar}	3.26
10	N	N	N	0	N	Gas-side C_{tar}	2.43
11	N	N	N	0	N	Gas-side C_{tar}	2.19
12	N	N	N	0	N	Gas-side C_{tar}	2.88
13	N	N	N	0	N	Gas-side C_{tar}	2.36
14	N	N	N	0	N	Gas-side C_{tar}	2.67
15	N	N	N	0	N	Water-loop I_{tox}	3.11
16	N	N	N	0	N	Gas-side C_{tar}	2.52
17	N	N	N	0	N	Gas-side C_{tar}	2.74
18	N	N	N	0	N	Gas-side C_{tar}	2.31
19	N	N	N	0	N	Gas-side C_{BTEX}	2.96
20	N	N	N	0	N	Gas-side C_{BTEX}	2.41
21	N	N	N	0	N	Gas-side I_N	1.67
22	Y	N	N	1	N	Gas-side C_{tar}	1.84
23	N	N	N	0	N	Water-loop I_{tox}	2.79
24	Y	Y	Y	3	Y	—	0.91
25	N	N	N	0	N	Gas-side C_{BTEX}	1.73
26	N	Y	N	1	N	Gas-side C_{BTEX}	1.08
27	N	N	N	0	N	Water-loop I_{tox}	3.34

In Table 5, "Y" indicates that all applicable Tier B criteria were satisfied for the corresponding biogenic-fraction category, whereas "N" indicates that one or more criteria were exceeded. The column "Robust (all Bio 40/50/60)" was assigned "Y" only when the corresponding condition remained feasible across all three biogenic-fraction categories. The column "n/3 feasible" indicates the number of biogenic-fraction categories for which all Tier B criteria were satisfied. The column "Primary limiting factor" identifies the criterion with the largest normalized exceedance relative to the Tier B threshold set, while "Max normalized exceedance" reports the highest normalized ratio among C_{tar}, C_{BTEX}, I_N, I_s, and I_{tox}.

2.7.2. Water-Loop Hazard Proxy, I_{tox}

To screen the manageability of the recirculated scrubber-water loop under sequential closed-loop operation, a dimensionless hazard proxy, I_{tox}, was defined. For each scrubber-water sample, class sums were calculated for phenolics (C_{phen}, mg L^{-1}), total PAHs (C_{PAH}, mg L^{-1}), and heavy PAHs (C_{hPAH}, mg L^{-1}; 4–6 ring subset). Reference concentrations C^*_{phen}, C^*_{PAH}, and C^*_{hPAH} were defined as the 75th percentile of the corresponding class sums across the full water dataset.

The composite hazard proxy was then calculated as follows:

 doi:10.20944/preprints202603.1829.v1

$$I_{tox} = 1.0 \ln\left(1 + \frac{C_{phen}}{C^*_{phen}}\right) + 2.0 \ln\left(1 + \frac{C_{PAH}}{C^*_{PAH}}\right) + 3.0 \ln\left(1 + \frac{C_{hPAH}}{C^*_{hPAH}}\right) \quad (2)$$

Non-detects were handled conservatively by substituting LOD/2 before class summation. I_{tox} was calculated for each analytical replicate (n = 3) and reported as mean ± SD.

The structure of I_{tox} was designed to represent water-loop manageability under sequential reuse rather than formal regulatory toxicity. The class weighting was selected to reflect the practical observation that phenolics often dominate the soluble organic burden and drive rapid deterioration of water-loop quality, whereas PAHs, and especially heavy PAHs, are more persistent and disproportionately relevant for treatment, purge demand, and handling burden. Logarithmic scaling was used to reduce excessive sensitivity to a single extreme class sum while preserving severity ranking across heterogeneous operating conditions. Tier-specific limits for I_{tox} (see Table 4) were applied jointly with the gas-side thresholds (see Table 3) to define feasibility and robustness.

2.7.3. Multi-Criteria Screening and Optimization Framing

Operating-regime selection was treated as a constrained multi-criteria problem in which gas-side cleanliness and water-loop manageability had to be satisfied simultaneously for a given end-use tier. In screening form, a DOE condition was considered feasible when all relevant tier-specific criteria were met. In optimization form, the same problem can be expressed as the minimization of a weighted composite objective subject to tier-specific constraints and a defined sequential cycling state.

The generic optimization framing used in this study is given below:

$$\min J = w_1 \frac{C_{tar}}{C_{tar,lim}} + w_2 \frac{C_{BTEX}}{C_{BTEX,lim}} + w_3 \frac{I_N}{I_{N,lim}} + w_4 \frac{I_S}{I_{S,lim}} + w_5 \frac{I_{tox}}{I_{tox,lim}} \quad (3)$$

subject to the tier-specific gas-side limits (Table 3), the water-loop limit (Table 4), and the cycling state defined for the corresponding DOE run (Table 1).

In the present work, the emphasis is placed on constraint-based feasibility mapping and on the identification of robust regimes across Bio 40/50/60 wt% rather than on optimization at a single average feed composition. Accordingly, the final interpretation combines threshold-based feasibility classification with the evaluation of gas–water trade-offs under sequential operation.

2.7.4. N/S Marker Indices in the Cleaned Pyrolysis Gas (GC–MS-Based Proxies)

To track heteroatom-related gas-quality constraints without performing bulk elemental gas speciation, nitrogen- and sulfur-containing aromatic compounds detected by GC–MS were used as marker-based indices. Two composite indices were defined for the cleaned gas: the nitrogen-heterocycle marker index I_N and the sulfur-aromatic marker index I_S.

Marker compounds were identified using retention-time consistency and qualifier/quantifier ion-ratio checks in SIM mode (see Section 2.5) and were quantified using the calibration and response-factor approach described in Section 2.6. Where a detected marker compound was not included in the calibrated target list, its concentration was estimated using the response factor of the closest calibrated compound within the same chemical class.

The nitrogen marker index, I_N, was defined as the class-sum concentration of detected N-heteroaromatic compounds, including pyridine-, alkyl-pyridine-, quinoline-, isoquinoline-, indole-, and related species. The sulfur marker index, I_S, was defined analogously as the class-sum concentration of detected sulfur-containing aromatics, including thiophene-, alkyl-thiophene-, benzothiophene-, dibenzothiophene-, and related compounds.

The mathematical definitions used for these two indices are given below:

$$I_N = \sum_{j \in N} C_j \quad (4)$$

 doi:10.20944/preprints202603.1829.v1

$$I_S = \sum_{k \in S} C_k \quad (5)$$

If marker compounds were detected in both stages of the SPA sampling train, their mass contributions were combined before normalization by sampled gas volume. Index values were calculated for each replicate (n = 3) and reported as mean ± SD.

These indices are intended as operational proxies for heteroatom-related gas-quality burdens relevant to corrosion, deposition, and emission precursor behavior. They are not interpreted as direct measures of total elemental nitrogen or sulfur in the gas phase.

2.8. Quality Assurance and Quality Control (QA/QC)

To ensure that the compound-resolved pollutant indices used in the feasibility screening were reproducible and analytically robust, the workflow incorporated QA/QC procedures for both the gas phase (SPA sampling followed by GC–MS) and the scrubber-water matrix (liquid–liquid extraction followed by GC–MS). QA/QC targeted three main risk categories: (i) sampling artefacts, including breakthrough, condensation losses, and contamination; (ii) extraction variability, recovery effects, and matrix-related bias; and (iii) instrument drift, carryover, and quantification errors. Unless stated otherwise, QA/QC criteria were applied on a batch basis. These procedures were designed to support reproducible calculation of C_{tar}, C_{BTEX}, I_N, I_S, and I_{tox} and, consequently, consistent tiered feasibility classification (see Table 3, Table 4, and Table 5).

2.8.1. Gas-Phase QA/QC

Field blanks and laboratory blanks were analyzed to identify background contamination and sorbent-derived artefacts. Field blanks consisted of fully assembled sampling trains exposed to routine handling without drawing process gas, whereas laboratory blanks consisted of unexposed sorbent cartridges. Target and marker compounds in blanks were required to remain below the limit of quantification (LOQ); otherwise, the analytical batch was flagged, and the affected compounds were treated conservatively by blank correction or censoring, as appropriate.

Breakthrough was evaluated using the two-stage SPA configuration by comparing analyte responses in the primary and backup stages. The backup-stage signal for representative marker compounds was required to remain ≤10% of the primary-stage mass to confirm negligible breakthrough. Samples exceeding this criterion were qualified and re-evaluated.

Replicate sampling was performed for each DOE condition and sampling point (n = 3). Sampling time, flow rate, and total sampled volume were documented for each replicate. The total sampled volume was required to remain within ±5% of the target value across replicates.

Compound identification was based on retention-time consistency and qualifier/quantifier ion-ratio checks in SIM mode. Confirmed identification required retention-time agreement within the validated analytical window and ion-ratio agreement within ±20% of the corresponding calibration-standard response.

2.8.2. Scrubber-Water QA/QC

Scrubber-water samples were collected in pre-cleaned amber glass bottles, cooled immediately, and stored protected from light until extraction. For sequential-cycle experiments, sampling was performed at predefined locations and cycle numbers to ensure comparability between runs and reuse states.

Surrogate standards representative of phenolic and PAH classes were added prior to extraction to monitor recovery. Matrix spikes and duplicate extractions were included within each analytical batch. Surrogate recoveries in the range of 70–130% were considered acceptable; values outside this range were retained but flagged. Duplicate extraction precision was evaluated using relative percent difference (RPD), with acceptance criteria of RPD ≤20% for class sums and ≤30% for samples close to the LOQ.

 doi:10.20944/preprints202603.1829.v1

Compound-specific LOD and LOQ values were recorded for the monitored analytes. Non-detects were handled conservatively by substituting LOD/2 before class summation and subsequent index calculation. Samples in which more than 50% of compounds within a given class were below the LOD were reported as semi-quantitative for that class.

2.8.3. Instrument Performance, Calibration, and Carryover Control

Quantification was performed using internal-standard normalization combined with external calibration, as described in Section 2.6. Calibration performance was accepted when the regression coefficient was $R^2 \geq 0.995$ and calibration residuals remained within ±15%, or within ±20% at the lowest calibration level.

Continuing calibration verification (CCV) injections were performed throughout each analytical sequence. CCV response factors were required to remain within ±15% of the expected value. When this criterion was not met, bracketed samples were reanalyzed or requantified after recalibration.

Carryover was monitored by injecting solvent blanks after high-concentration samples. Carryover for key analytes was required to remain below the LOQ. If carryover exceeded this threshold, additional injector and syringe rinsing steps were performed and blank injections were repeated before further sample analysis.

2.8.4. Data Integrity and Reproducibility

Each sample was assigned a unique identifier linking the dataset to DOE condition, RDF biogenic-fraction category, cycling level, replicate number, sampling volume, extraction batch, and GC–MS sequence order. Raw chromatograms, integration parameters, calibration and CCV records, and calculation sheets used for class sums and derived indices were archived to support reproducibility and retrospective verification of all reported results. The archived dataset also included the intermediate calculations used for tiered feasibility screening and robustness classification (see Table 5).

2.9. Reproducibility Note

The results reported in this study were generated from compound-resolved GC–MS measurements of cleaned RDF pyrolysis gas and recirculated scrubber water obtained under a 27-run L27 DOE matrix and three RDF biogenic-fraction categories. The operating matrix and factor definitions are provided in Table 1, while the screening thresholds and feasibility outcomes are reported in Table 3, Table 4, and Table 5. The cleaned-gas indicators and water-loop indices were calculated from the equations, class definitions, and analytical rules described in Sections 2.5–2.8 (see Equation (2), Equation (3), Equation (4), and Equation (5). All feasibility labels and robustness classifications were derived directly from the measured or response-factor-estimated compound concentrations and the tier-specific screening thresholds applied in this study.

3. Results and Discussion

3.1. Compound-Class Fingerprints Across the DOE Operating Space

Across the 27-run DOE, the post-scrubber (“cleaned”) gas exhibited a broad span of pollutant burdens, confirming strong class-dependent sensitivity to both pyrolysis severity and direct wet scrubbing. Across the full operating space and biogenic-fraction categories, the tar proxy ranged from 1.71 to 5.47 g Nm^{-3}, whereas the BTEX class sum ranged from 0.46 to 2.50 g Nm^{-3}. The N-heterocycle and S-aromatic marker indices spanned 19.4–48.3 mg Nm^{-3} and 26.0–65.6 mg Nm^{-3}, respectively, indicating that heteroatom-related constraints remained relevant even when condensable carryover was reduced (Figure 3).

 doi:10.20944/preprints202603.1829.v1

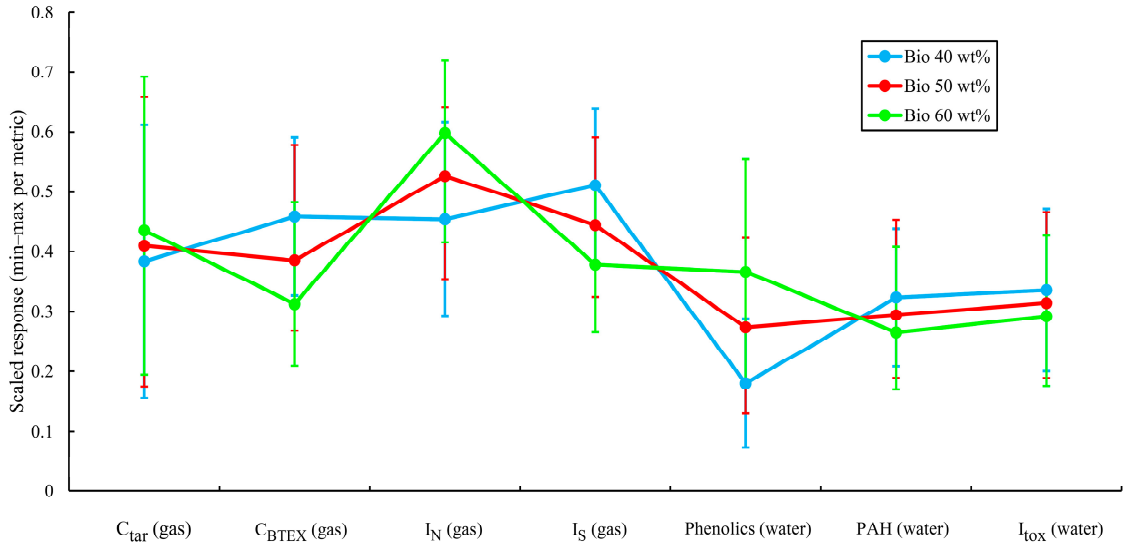

Figure 3. Biogenic-fraction profiles across key gas- and water-phase indices (median ± IQR).

Scrubbing intensity shifted semi-volatile and condensable species from the gas phase into the aqueous loop. Increasing the liquid-to-gas ratio from 0.5 to 2.0 L m^{-3} reduced the median gas-phase tar proxy from 3.69 to 2.84 g Nm^{-3} (approximately 23%) and reduced the median BTEX burden from 1.50 to 1.10 g Nm^{-3} (approximately 27%). This gas-side improvement occurred alongside a marked increase in water-loop loading, as the median phenolics concentration in scrubber water increased from 227 to 408 mg L^{-1} (approximately 80%), consistent with enhanced transfer into the recirculating liquid phase. Lower scrubber-water temperature further strengthened condensation-driven capture. In particular, decreasing Tscrub from 50 to 20 °C reduced the median BTEX burden from 1.74 to 0.895 g Nm^{-3} (approximately 49%).

Taken together, these results show that stronger wet scrubbing improved cleaned-gas quality, but the response was strongly compound-class-dependent and was accompanied by increased pollutant transfer to the recirculating water phase. This behavior is important for the interpretation of downstream feasibility, because reduced gas-phase tar or BTEX does not necessarily imply a lower overall process burden when the water loop is operated in closed recirculation. The observed fingerprints, therefore, support the use of compound-class indices rather than a single total-tar metric and provide the basis for the accumulation analysis presented in Section 3.2.

3.2. Accumulation During Sequential Closed-Loop Operation (5/10/15 Consecutive Cycles)

Sequential reuse of the same scrubber-water inventory over 5, 10, and 15 consecutive pyrolysis cycles resulted in systematic accumulation of organic pollutants in the aqueous phase. Across the dataset, the median phenolics concentration increased from 172.5 mg L^{-1} at 5 cycles to 458.0 mg L^{-1} at 15 cycles, corresponding to an approximately 2.7-fold increase. Over the same cycling interval, the median water-phase PAH sum increased from 2.09 to 8.64 mg L^{-1}, i.e., by approximately 4.1-fold, indicating that extended closed-loop operation disproportionately intensified PAH-related loading (Figure 4). Consistently, the composite water-loop hazard proxy, I_{tox}, increased from a median of 3.62 at 5 cycles to 9.36 at 15 cycles (approximately +159%), demonstrating that water-loop constraints became progressively more restrictive with increasing reuse state (Figure 5).

 doi:10.20944/preprints202603.1829.v1

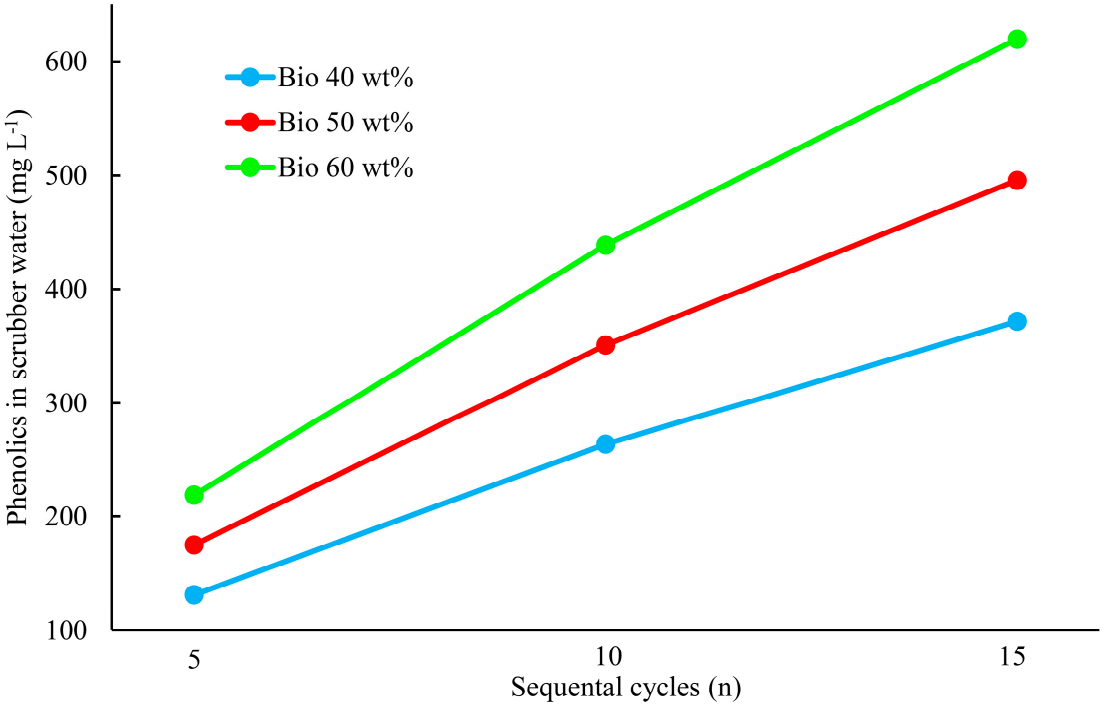

Figure 4. Effect of sequential closed-loop reuse (5, 10, and 15 consecutive cycles) on phenolics and total PAHs in scrubber water.

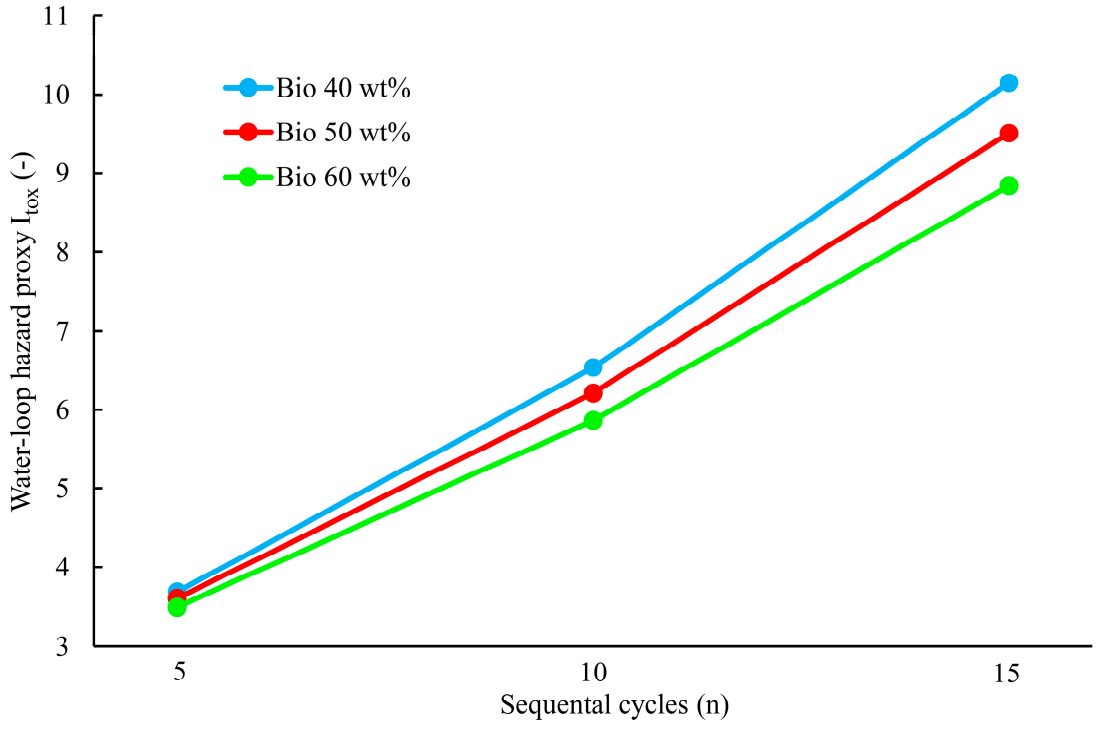

Figure 5. Effect of sequential closed-loop reuse (5, 10, and 15 consecutive cycles) on the composite water-loop hazard proxy, I_{tox}.

The stronger relative increase in PAHs than in total phenolics suggests that prolonged recirculation did not merely increase total dissolved organic burden, but also shifted the retained pollutant inventory toward more persistent and higher-molecular-weight species. This pattern is consistent with a "heavification" trend in the recirculating liquid phase, in which repeated transfer

 doi:10.20944/preprints202603.1829.v1

of condensable organics and limited removal under closed-loop operation promote enrichment of less volatile aromatic fractions. From an implementation perspective, this distinction is important because a water loop that remains manageable at 5 cycles may approach or exceed practical hazard limits at 10–15 cycles even when gas-side cleaning performance appears improved.

These results show that sequential cycling must be treated as a coupled operational constraint rather than as a secondary housekeeping variable. In practical terms, more aggressive gas cleaning can improve the cleaned-gas profile while simultaneously accelerating water-loop deterioration under reuse. The observed increase in I_{tox} therefore provides direct support for the tiered feasibility framework introduced in Section 2.7, where operating windows are defined jointly by gas-side cleanliness and water-loop manageability. This coupling is examined more explicitly in the end-use screening results presented in the following subsection.

3.3. End-Use Screening: Boiler vs. ICE-CHP vs. Microturbine

Tiered end-use screening showed that feasibility was rarely limited by a single pollutant class and that the feasible operating space contracted sharply as end-use requirements became more stringent. This pattern is illustrated by the cleaned-gas screening map in Figure 6, where the Tier B limits are shown in the C_{tar}–C_{BTEX} plane.

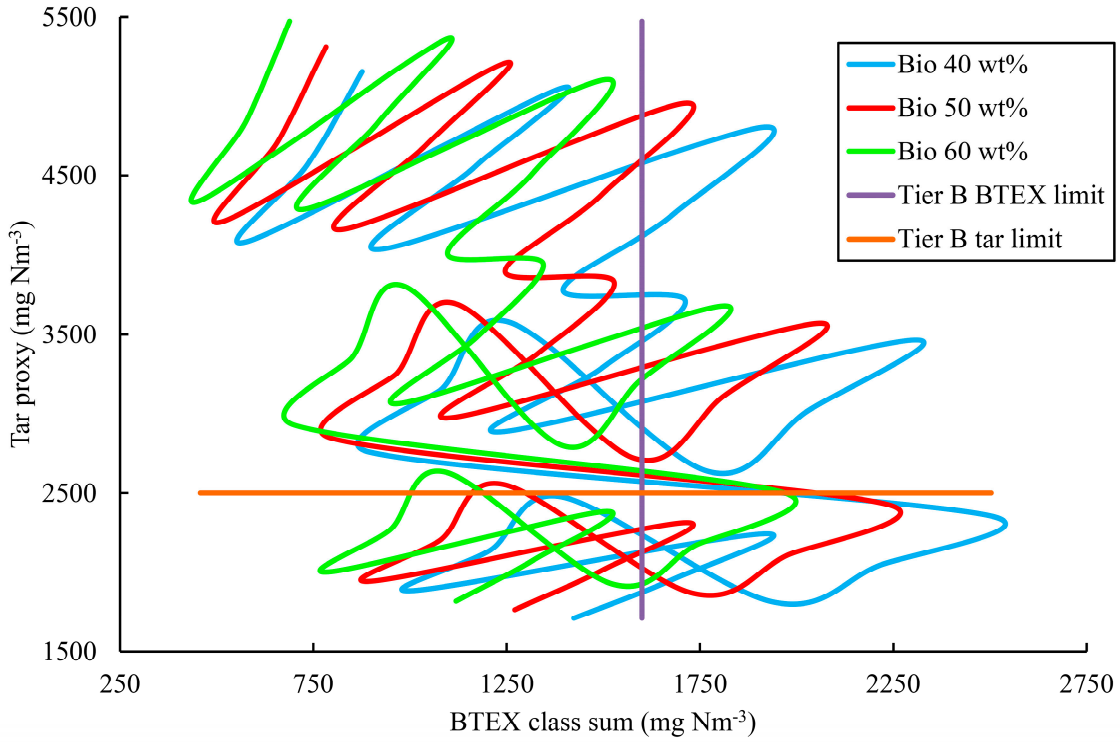

Figure 6. Cleaned-gas screening map for the Tier B target set.

Under the Tier A target set, boiler-grade operation remained comparatively tolerant. Across the tested operating space, 23 of the 27 DOE conditions remained robust across the Bio 40/50/60 wt% categories, indicating that moderate variation in feed biogenic fraction did not substantially compromise feasibility when the end-use tolerance to residual pollutant burden was relatively high. In contrast, Tier B screening for ICE-CHP was markedly more restrictive. Only one condition, Run 24, remained robust across all three biogenic-fraction categories when both the Tier B gas-side targets and the Tier B water-loop constraint were applied simultaneously. Tier C, corresponding to microturbine-oriented utilization, was the most restrictive: no DOE condition satisfied the full Tier C target set across Bio 40/50/60 wt% within the tested operating window.

 doi:10.20944/preprints202603.1829.v1

Taken together, these results show that stronger gas cleaning alone is insufficient to define a practically feasible operating regime. As end-use requirements tighten, pollutant redistribution to the recirculating scrubber-water loop becomes an increasingly important limiting factor, particularly under sequential cycling. Thus, the feasible set contracts not only because the cleaned gas must be substantially cleaner, but also because the water loop becomes progressively more difficult to manage under the same conditions. This hierarchy provides the basis for identifying robust operating windows across process severity, scrubber settings, and feed variability, as discussed in Section 3.4.

3.4. Operating Windows and Robust Regimes Across Bio 40–60 wt% and Sequential Cycling

Table 5 summarizes the Tier B (ICE-CHP) operating-window screening outcomes for the 27 DOE conditions evaluated across the three RDF biogenic-fraction categories (Bio 40/50/60 wt%) and the defined sequential cycling states (5, 10, and 15 consecutive cycles using the same scrubber-water inventory). Feasibility was defined by simultaneous satisfaction of the Tier B gas-side thresholds and the Tier B water-loop criterion, whereas robustness required feasibility to be retained across all three biogenic-fraction categories at the cycling level associated with the corresponding DOE run.

Under the Tier B target set, only one condition, Run 24, remained robust across Bio 40/50/60 wt% within the tested configuration. This regime combined high pyrolysis temperature (520 °C), moderate residence time (15 min), high scrubbing intensity (L/G = 2.0 L m^{-3}), low scrubber-water temperature (20 °C), and low cycling level (5 cycles). In practical terms, this operating window achieved a favorable compromise in which gas-side condensables and BTEX were sufficiently suppressed while the water-loop hazard remained below the Tier B limit (Figure 7). By contrast, most other DOE conditions failed because of either residual gas-side burdens, particularly tar and BTEX, or excessive water-loop hazard under more extended cycling.

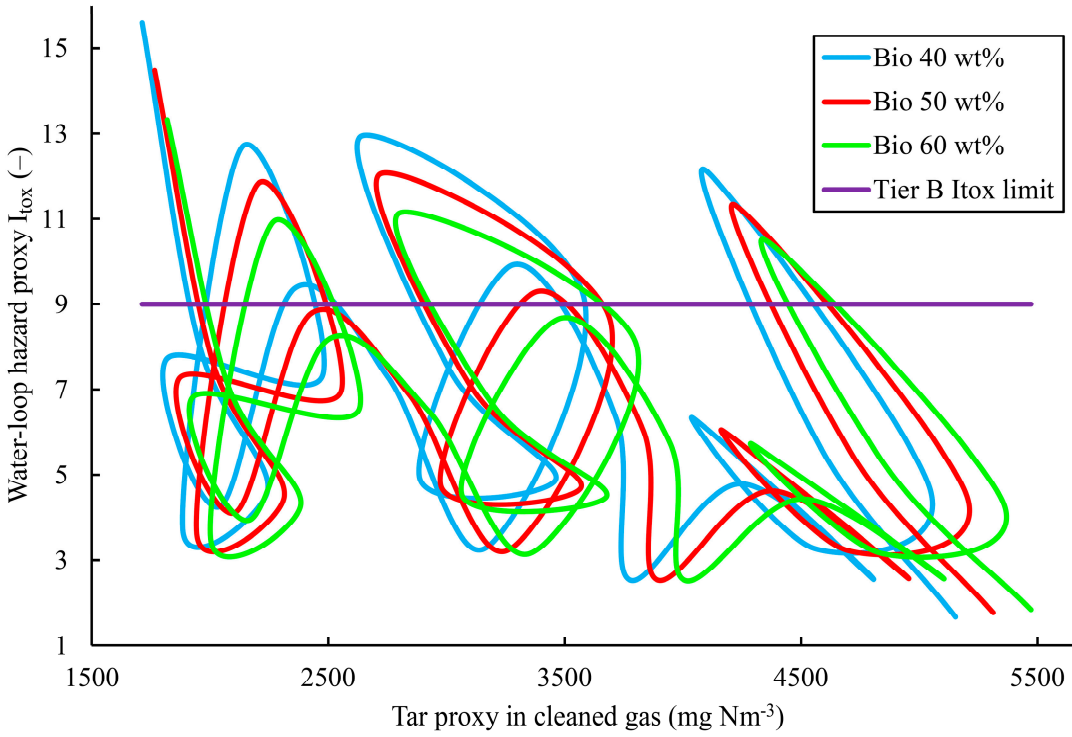

Figure 7. Coupled gas–water feasibility constraint for the Tier B target set, shown as cleaned-gas tar proxy versus water-loop hazard proxy.

This behavior highlights that the feasible ICE-CHP operating window is determined by a coupled gas–water constraint rather than by cleaned-gas quality alone. Figure 7 illustrates this coupling by plotting the cleaned-gas tar proxy against the water-loop hazard proxy under the Tier B

 doi:10.20944/preprints202603.1829.v1

limit, showing how sequential cycling can collapse the feasible region even when gas-side indices improve. In this sense, operating severity and scrubber setpoints cannot be interpreted independently of the cycling state: conditions that appear favorable from a gas-cleaning perspective may still become infeasible once pollutant accumulation in the recirculating water loop is taken into account.

A brief sensitivity check, based on ±20% variation of the Tier B I_{tox} limit and modest reweighting of the water-loop class coefficients, did not change the identity of the robust Tier B regime within the tested operating space. This result indicates that the "single robust regime" outcome is not merely an artefact of a narrowly chosen threshold, but reflects the broader structure of the coupled screening constraints. The corresponding sensitivity ranking is shown in Figure 8.

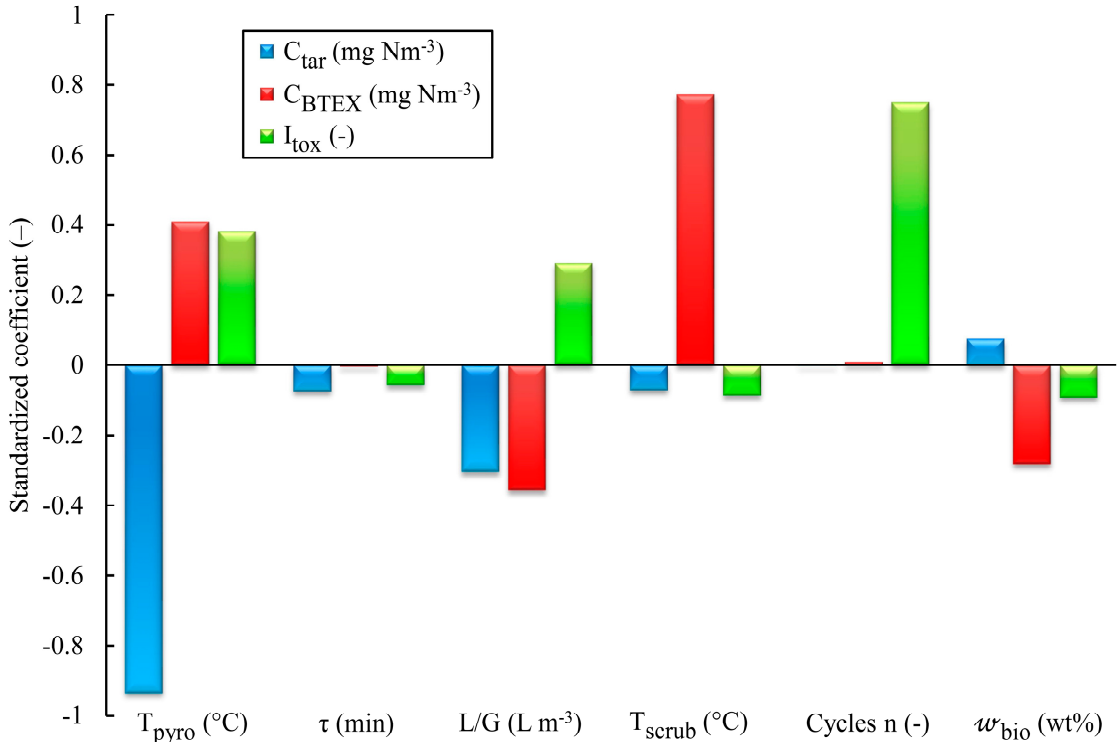

Figure 8. Sensitivity ranking of the Tier B screening outcome based on standardized coefficients from the linear model.

From an application perspective, the contrast between tiers remains clear. Boiler-grade operation (Tier A) retains a substantially broader feasible set, indicating that many conditions remain acceptable for direct heat use even when both gas-side and water-loop effects are considered. By contrast, the absence of any fully feasible Tier C condition confirms that the tested direct wet-scrubbing configuration is insufficient by itself to achieve microturbine-grade requirements within the explored operating window. Achieving such a target would likely require either additional downstream gas cleaning, more aggressive water-loop control, or a different scrubbing architecture.

3.4.1. Practical Design Rules for Integrated RDF Pyrolysis–Wet Scrubbing Systems

The combined screening results allow several practical design rules to be formulated for integrated RDF pyrolysis–wet scrubbing systems operated with closed-loop water reuse. First, gas-side improvement should not be interpreted in isolation. Across the tested operating space, stronger wet scrubbing improved the cleaned-gas profile, but this benefit was frequently offset by faster deterioration of the recirculating water loop. As a result, process optimization based only on cleaned-gas tar or BTEX is insufficient for identifying practically feasible operating regimes (see Figure 7).

Second, the most favorable ICE-CHP-oriented regime within the tested configuration was associated with a combination of high pyrolysis temperature, moderate residence time, high

 doi:10.20944/preprints202603.1829.v1

scrubbing intensity, low scrubber-water temperature, and limited water-loop reuse. This indicates that efficient condensation and capture of problematic gas-phase species can support engine-oriented targets, but only when the accumulated burden in the scrubber water remains below a manageable threshold. In practice, this means that aggressive scrubbing should be paired with active water-loop management rather than treated as a stand-alone solution.

Third, the results highlight a clear end-use hierarchy. For direct heat production, the feasible operating space remained broad, suggesting that comparatively simple gas cleaning may be sufficient for boiler-grade deployment. For ICE-CHP, however, the feasible window narrowed sharply and required simultaneous control of both gas-side and water-side burdens. For microturbine-oriented use, the present direct wet-scrubbing configuration was not sufficient within the explored operating window, indicating that additional downstream polishing or a modified gas-cleaning architecture would be required (see Figure 6 and Figure 7).

Overall, the present results suggest that robust process design for RDF pyrolysis should be based on coupled gas–water constraints, explicit cycling limits, and end-use-specific screening rather than on a single gas-quality metric.

3.5. System-Level Penalties of Stricter Wet Scrubbing (Order-of-Magnitude Perspective)

From an energy-systems perspective, stricter gas-quality targets impose non-negligible balance-of-plant penalties in addition to the pollutant-control benefits discussed above. Increasing the liquid-to-gas ratio raises the recirculating liquid flow rate and therefore the pumping demand, which can be approximated as

$$P_{pump} \approx \Delta_{p_{loop}} \times \dot{V}_L / \eta \quad (6)$$

where P_{pump} is the pump power demand, $\Delta_{p_{loop}}$ is the overall hydraulic pressure drop of the liquid recirculation loop, $\dot{V}_L$ is the liquid volumetric flow rate, and η is the overall pump efficiency. Likewise, maintaining a low scrubber-water temperature, such as 20 °C, requires additional cooling duty, which can be approximated as

$$\dot{Q}_{cool} \approx \dot{m}_L \times c_p \times (T_{in} - T_{scrub}) \quad (7)$$

where $\dot{Q}_{cool}$ is the required cooling duty, $\dot{m}_L$ is the recirculating liquid mass flow rate, c_p is the specific heat capacity of the liquid phase, T_{in} is the inlet temperature of the liquid entering the cooling unit, and T_{scrub} is the scrubber-water set temperature. This expression represents a first-order sensible cooling estimate and does not explicitly include latent heat effects, gas-side cooling, or other secondary thermal loads. Both penalties increase directly with liquid circulation rate and with the temperature lift required for effective condensation-driven capture.

Sequential closed-loop reuse introduces a third operational burden: purge/make-up demand or side-stream treatment to prevent excessive escalation of I_{tox} at extended cycling states. In practical terms, the transition from Tier A to Tier B and Tier C therefore reflects not only stricter gas-cleanliness requirements, but also the cumulative system-level cost of pumping, cooling, and water-loop management. This is important because operating conditions that appear attractive from the standpoint of cleaned-gas quality alone may become less favorable once these auxiliary penalties are considered.

Taken together, these order-of-magnitude considerations support expressing deployment guidance as two practical operating envelopes: (i) a baseline feasible regime under limited cycling and without aggressive water-loop intervention, and (ii) an extended regime that becomes achievable only when explicit purge/make-up, side-stream treatment, or other active water-loop control measures are incorporated into system operation.

 doi:10.20944/preprints202603.1829.v1

4. Conclusions

This study evaluated RDF pyrolysis coupled with direct wet scrubbing and closed-loop scrubber-water reuse across a 27-run DOE covering pyrolysis severity, scrubber operating conditions, and three RDF biogenic-fraction categories (Bio 40/50/60 wt%). Across the tested operating space, the cleaned-gas tar proxy ranged from 1.71 to 5.47 g Nm^{-3}, whereas the BTEX class sum ranged from 0.46 to 2.50 g Nm^{-3}, confirming strong compound-class-dependent variability of the post-scrubber gas.

Increasing the liquid-to-gas ratio from 0.5 to 2.0 L m^{-3} reduced the median gas-phase tar proxy from 3.69 to 2.84 g Nm^{-3} (approximately 23%) and the median BTEX burden from 1.50 to 1.10 g Nm^{-3} (approximately 27%), while lowering scrubber-water temperature from 50 to 20 °C reduced the median BTEX burden from 1.74 to 0.895 g Nm^{-3} (approximately 49%). However, these gas-side gains were accompanied by increased pollutant transfer to the recirculating water phase, with median phenolics in scrubber water increasing from 227 to 408 mg L^{-1} (approximately 80%) under stronger scrubbing conditions.

Sequential reuse of the same scrubber-water inventory over 5, 10, and 15 consecutive cycles resulted in systematic accumulation of organic pollutants. The median phenolics concentration increased from 172.5 to 458.0 mg L^{-1} (approximately 2.7-fold), the median water-phase PAH sum increased from 2.09 to 8.64 mg L^{-1} (approximately 4.1-fold), and the median water-loop hazard proxy, I_{tox}, increased from 3.62 to 9.36 (approximately +159%). These results show that water-loop deterioration under closed-loop operation is a central process constraint rather than a secondary operational issue.

End-use screening demonstrated a clear hierarchy of feasible operating space. Boiler-grade operation (Tier A) remained robust for 23 of the 27 tested DOE conditions, whereas under the Tier B ICE-CHP target set only one condition (Run 24) remained robust across all three RDF biogenic-fraction categories. No fully feasible condition was identified for the Tier C microturbine-oriented target set within the explored configuration.

Overall, the results show that operating windows for RDF pyrolysis with wet scrubbing must be defined by coupled gas–water constraints rather than by cleaned-gas metrics alone. Robust process design therefore requires end-use-specific screening, explicit control of sequential cycling, and active management of the recirculating water loop when stricter gas-quality targets are pursued.

Author Contributions: Conceptualization, S.O. and A.P.; methodology, S.O. and A.P.; investigation, S.O. and A.P.; data curation, S.O. and A.P.; formal analysis, S.O. and A.P.; visualization, A.P.; supervision, S.O.; writing—original draft preparation, A.P. and S.O.; writing—review and editing, S.O. and A.P. All authors have read and agreed to the published version of the manuscript.

Funding: This research was funded by DAUGAVPILS UNIVERSITY, grant number 14-95/2026/15.

Data Availability Statement: The data presented in this study are available from the corresponding author upon reasonable request. The dataset includes the L27 operating matrix, compound-resolved GC–MS results for the cleaned gas and recirculated scrubber water, and the calculated screening indices used for tiered feasibility classification.

Conflicts of Interest: The authors declare no conflicts of interest.

Abbreviations

The following abbreviations are used in this manuscript:

RDF	refuse-derived fuel
DOE	design of experiments
BTEX	benzene, toluene, ethylbenzene, and xylenes
PAHs	polycyclic aromatic hydrocarbons
GC–MS	gas chromatography–mass spectrometry
SPA	solid-phase adsorption

 doi:10.20944/preprints202603.1829.v1

ICE-CHP internal combustion engine combined heat and power

References

1. Alfè, M.; Gargiulo, V.; Di Capua, R.; Ragozzino, E.; Ammendola, P. Pyrolysis and Gasification of a Real Refuse-Derived Fuel: Characterization and Reactivity of Chars. Molecules 2022, 27, 8114. https://doi.org/10.3390/molecules27238114.
2. Kusz, B.; Junga, R.; Kujawski, W. Pyrolysis of RDF and Catalytic Decomposition of the Produced Tar in a Char Bed Secondary Reactor as an Efficient Source of Syngas. Processes 2022, 10, 90. https://doi.org/10.3390/pr10010090.
3. Jayanarasimhan, A.; et al. Tar Formation in Gasification Systems: A Holistic Review of Remediation Approaches and Removal Methods. ACS Omega 2024. https://doi.org/10.1021/acsomega.3c04425.
4. Milne, T.A.; Evans, R.J.; Abatzoglou, N. Biomass Gasifier "Tars": Their Nature, Formation, and Conversion. NREL Report, 1998.
5. Asadullah, M. Biomass Gasification Gas Cleaning for Downstream Applications: A Comparative Critical Review. Renew. Sustain. Energy Rev. 2014, 40, 118–132. https://doi.org/10.1016/j.rser.2014.07.093.
6. Han, J.; Kim, H. The Reduction and Control Technology of Tar during Biomass Gasification/Pyrolysis: An Overview. Renew. Sustain. Energy Rev. 2008, 12, 397–416. https://doi.org/10.1016/j.rser.2006.07.015.
7. Devi, L.; Ptasinski, K.J.; Janssen, F.J.J.G. A Review of the Primary Measures for Tar Elimination in Biomass Gasification Processes. Biomass Bioenergy 2003, 24, 125–140. https://doi.org/10.1016/S0961-9534(02)00102-2.
8. Pučkins, A.I.; Osipovs, P.S.; Osipovs, S.D. Method for the Determination of Tar Produced from the Pyrolysis of Used Tires. Int. J. Energy Clean Environ. 2024, 25(1), 69–82. https://doi.org/10.1615/InterJEnerCleanEnv.2023047672.
9. Hasler, P.; Nussbaumer, Th. Gas Cleaning for IC Engine Applications from Fixed Bed Biomass Gasification. Biomass Bioenergy 1999, 16, 385–395. https://doi.org/10.1016/S0961-9534(99)00018-5.
10. Din, Z.U.; Zainal, Z.A. Tar Reduction Mechanism via Compression of Producer Gas. J. Clean. Prod. 2018, 184, 1–11. https://doi.org/10.1016/j.jclepro.2018.02.198.
11. Susastriawan, A.A.P.; Saptoadi, H.; Purnomo. Biomass Gasifier–Internal Combustion Engine System: Review of Literature. Energy Sources Part A 2021. https://doi.org/10.1080/19397038.2020.1821404.
12. Aguado, R.; Vera, D.; Jurado, F.; et al. An Integrated Gasification Plant for Electric Power Generation from Wet Biomass: Toward a Sustainable Production in the Olive Oil Industry. Biomass Convers. Biorefin. 2025, 15, 29893–29912. https://doi.org/10.1007/s13399-021-02231-0.
13. Biomass Engineering Ltd. Development of a Micro-Turbine Plant to Run on Gasifier Producer Gas; B/U1/00762/REP; URN 04/1804; Biomass Engineering Ltd.: Newton-le-Willows, UK, 2004.
14. Oakey, J.E.; Simms, N.J.; Kilgallon, P. Gas Turbines: Gas Cleaning Requirements for Biomass-Fired Systems. Mater. Res. 2004, 7, 17–25. https://doi.org/10.1590/S1516-14392004000100004.
15. Woolcock, P.J.; Brown, R.C. A Review of Cleaning Technologies for Biomass-Derived Syngas. Biomass Bioenergy 2013, 52, 54–84. https://doi.org/10.1016/j.biombioe.2013.02.036.
16. Lotfi, S.; Ma, W.; Austin, K.; Kumar, A. A Wet Packed-Bed Scrubber for Removing Tar from Biomass Producer Gas. Fuel Process. Technol. 2019, 193, 197–203. https://doi.org/10.1016/j.fuproc.2019.05.024.
17. Balas, M.; Lisy, M.; Kubicek, J.; Pospisil, J. Syngas Cleaning by Wet Scrubber. WSEAS Trans. Heat Mass Transf. 2014, 9, 195–204.
18. Osipovs, S.D.; Pučkins, A.I.; Mežaraupe, S.; Lazdāns, D. Determination of Pollutants in Industrial Water Used for Cooling Gases in Waste Pyrolysis Process. Int. J. Energy Clean Environ. 2022, 23, 61–73.
19. Huber, M.; et al. Tar Conversion and Recombination in Steam Gasification of Biogenic Residues: The Influence of a Countercurrent Flow Column in Pilot- and Demonstration-Scale. Fuel 2024, 364, 131068. https://doi.org/10.1016/j.fuel.2024.131068.
20. Rabou, L.P.L.M.; Balegedde Ramachandran, R.P.; Hoeben, W.F.L.M.; de Jong, W.; Kersten, S.R.A.; Leijenhorst, E.J.; Kumar, K.; Mourao Vilela, C.F.; Nanou, P.; van Oijen, J.A.; Pemen, A.J.M.; Rindt, C.C.M.; van Rossum, G.; Verhoeven, L.M. EOS-LT Consortium Biomass Gasification and Gas Cleaning Final Report

 doi:10.20944/preprints202603.1829.v1

2007–2011; ECN-E--12-010; Energy Research Centre of the Netherlands (ECN): Petten, The Netherlands, 2012.

21. Raman, P.; Ram, N.K. Performance Analysis of an Internal Combustion Engine Operated on Producer Gas, in Comparison with the Performance of the Natural Gas and Diesel Engines. Energy 2013, 63, 317–333. https://doi.org/10.1016/j.energy.2013.10.033.
22. De Oliveira, D.C.; et al. Tar Removal from Biomass-Derived Syngas for Hydrogen Production: Oil Absorption Process Considering Brazilian Sources. Int. J. Hydrogen Energy 2025, in press. https://doi.org/10.1016/j.ijhydene.2024.02.212.
23. Maniatis, K.; Beenackers, A.A.C.M. Tar Protocols. Biomass Bioenergy 2000, 18, 1–4. https://doi.org/10.1016/S0961-9534(99)00072-0.
24. X. van Paasen, S.V.B.; Kiel, J.H.A.; Neeft, J.P.A.; Knoef, H.A.M.; Buffinga, G.J.; Zielke, U.; Sjöström, K.; Brage, C.; Hasler, P.; Simell, P.A.; Suomalainen, M.; Dorrington, M.A.; Thomas, L. Guideline for Sampling and Analysis of Tar and Particles in Biomass Producer Gases; ECN-C--02-090; Energy Research Centre of the Netherlands (ECN): Petten, The Netherlands, 2002
25. van de Kamp, W.L.; de Wild, P.J.; Knoef, H.A.M.; Neeft, J.P.A.; Kiel, J.H.A. Tar Measurement in Biomass Gasification: Standardisation and Supporting R&D; ECN-C--06-046; Energy Research Centre of the Netherlands (ECN): Petten, The Netherlands, 2006.
26. IEA Bioenergy Task 33. Gas Analysis in Gasification of Biomass and Waste. Guideline Report—Document 1; IEA Bioenergy: 2018.
27. Horvat, A.; Kwapinska, M.; Abdel Karim Aramouni, N.; Leahy, J.J. Solid Phase Adsorption Method for Tar Sampling—How Post Sampling Treatment Affects Tar Yields and Volatile Tar Compounds? Fuel 2021, 291, 120059. https://doi.org/10.1016/j.fuel.2020.120059.
28. Osipovs, S. Sampling of Benzene in Tar Matrices from Biomass Gasification Using Two Different Solid-Phase Sorbents. Anal. Bioanal. Chem. 2008, 391, 1409–1417. https://doi.org/10.1007/s00216-007-1809-7.
29. Osipovs, S. Use of Two Different Adsorbents for Sampling Tar in Gas Obtained from Peat Gasification. Int. J. Environ. Anal. Chem. 2009, 89, 871–880. https://doi.org/10.1080/03067310802592755.
30. Osipovs, S. Comparison of Efficiency of Two Methods for Tar Sampling in the Syngas. Fuel 2013, 103, 387–392. https://doi.org/10.1016/j.fuel.2012.05.021.
31. Pučkins, A.; Osipovs, S. Selection of the Second Adsorbent for Sampling Volatile Organic Compounds in the Biomass Gasification Tar Using Solid-Phase Adsorption. ACS Omega 2023, 8(46), 43993-43998. https://doi.org/10.1021/acsomega.3c06097.
32. Pučkins, A.I.; Osipovs, S.D.; Stašāns, M. Separate Identification of Phenolic and Polyaromatic Fractions in the Course of Tar Analysis. Int. J. Energy Clean Environ. 2025, 26, 33-49. https://doi.org/10.1615/InterJEnerCleanEnv.2024054691
33. Osipovs, S.D.; Pučkins, A.I.; Kirilova, E.M.; Soms, J. Development of a Solid Phase Adsorption Analysis Method for the Measurement of Nitrogen Organic Compounds in Producer Gas. Biomass Convers. Biorefin. 2023, 13(12), 10551–10560. https://doi.org/10.1007/s13399-021-01970-4.